Low complexity design of variable bandedge linear phase FIR filters with sharp transition band

Yu, Ya Jun; Lim, Yong Ching; Shi, Dong

2009

Yu, Y. J., Lim, Y. C., & Shi, D. (2009). Low-Complexity Design of Variable Bandedge Linear Phase FIR Filters With Sharp Transition Band. IEEE Transactions On Signal Processing. 57(4), 1328-1338.

https://hdl.handle.net/10356/91837

https://doi.org/10.1109/TSP.2008.2010597

Low-Complexity Design of Variable Bandedge Linear Phase FIR Filters With Sharp Transition Band

Ya Jun Yu, *Member, IEEE*, Yong Ching Lim, *Fellow, IEEE*, and Dong Shi, *Student Member, IEEE*

***Abstract*—This paper presents a very low-complexity design of variable bandedge linear phase finite-impulse-response (FIR) filters with fixed sharp transition width. The idea is to first decompose the input signal into several channels in the frequency domain. The channel(s) involved with the transition band of the variable filter due to the variation of the bandedge is (are) shaped to produce the required transition band, and then summed up with the channels involved with the passband of the variable filter to produce the required frequency response. The proposed variable filter has extremely low complexity when the transition band is sharp, if compared with other techniques such as the Farrow structure. It is possible that the computational complexity of the variable filter is even lower than that of a corresponding fixed filter with the same transition width and ripple specifications implemented in its direct form.**

***Index Terms*—Fast filter bank, finite-impulse-response filter, frequency-response masking, variable digital filters.**

I. Introduction

VARIABLE digital filters have wide applications in telecommunication, medical instrument, and digital radios. The variable characteristics of digital filters mainly present on the variable frequency response, such as variable cutoff/bandedge frequency [1]–[10], and controllable fractional delay [11]–[15].

Many researches have studied digital filters with variable cutoff/bandedge frequency, where the transition width is fixed, but the cutoff frequency, or the bandedges are variable over a range of frequencies. The techniques of interest are generally those constructing the filter in such a way that the cutoff/bandedge frequency is controlled by only a single parameter. Existing techniques include: First, a transform approach was proposed by Schuessler and Winkelnkemper [1] in 1970. In this approach, each delay element of a prototype filter is replaced by a first-order all pass network to transform the frequency. The resulting filter then has an identical frequency response as that of the prototype filter, but on a distorted frequency scale. Oppenheim *et al.* [2] proposed a new class of transformation based on the above technique, so that the resulting impulse response of the filter is finite and the phase of the filter is linear. Further studies and extension of this technique were presented in [3]–[5]. Transformation approach generally increases the filter length, and special filter structure is employed.

In the second class of technique proposed by Jarske *et al.* [6], the variable filter coefficients are approximated by simple sine functions of the cutoff frequency. Due to the direct control of the filter coefficients, the length of the filter remains unchanged when it is made variable. However, the direct approximation of coefficient affects the coefficient precision resulting in the deterioration of the magnitude response; the best stopband attenuation achievable by this method is not more than 40 dB.

Recently, the Farrow structure [11] has received great attention in realizing variable bandedge filters [7]–[10]. In this technique, the overall filter transfer function is a weighted linear combination of a few fixed linear phase FIR filters; the weights are polynomial of the bandedge frequency, and thus are easy to update. However, the computational complexity of the Farrow structure is very high.

A straightforward but practical method to implement variable bandedge FIR filter is to use a set of over-designed fixed filters, each having several times sharper transition band than that required by the variable filter. Thus, each filter is taking care of only part of the variable frequency regions [16]. At any moment of the operation, only one of the filters is used. Due to the over-design of the filters, however, the computational complexity of the filters are high, especially when the variable filter requires sharp transition band.

It is well known that the computational complexity in terms of the number of multiplications is inversely proportional to the transition width. When the filters are made variable, the complexity is at least as high as that of their corresponding directly implemented fixed filters with the same transition widths. Variable filters employing the Farrow structure and over-designed set of filters have even higher computational complexity.

In contrast to the traditional variable filters that vary the bandedge of the frequency response of the filters, this paper proposes a method to efficiently shift the input signal frequency spectrum. The frequency-shifted signal is shaped by a filter with a fixed bandedge, and then shifted back to its original frequency region. The proposed technique achieves the same effect of varying the bandedge by shifting the signal along the frequency axis. By making use of the low-complexity techniques in fixed filter design, the overall computational complexity of the variable filter may even be lower than that of a fixed filter with the same transition width and ripple requirements implemented in its direct form.

The remaining of the paper is organized as follows. Section II reviews the low-complexity techniques on the design of

Manuscript received February 22, 2008; revised February 22, 2008. First published December 09, 2008; current version published March 11, 2009. The associate editor coordinating the review of this manuscript and approving it for publication was Dr. Soontorn Oraintara. This project is supported in part by Nanyang Technological University (NTU) and Temasek Laboratory at NTU.

The authors are with the School of Electrical and Electronic Engineering, Nanyang Technological University, Singapore (e-mail: eleyuyj@pmail.ntu.edu.sg; elelimyc@pmail.ntu.edu.sg; shid0001@ntu.edu.sg).

Digital Object Identifier 10.1109/TSP.2008.2010597

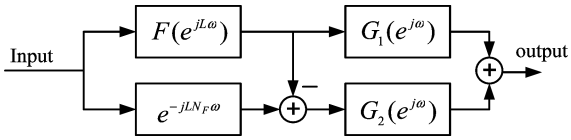

Fig. 1. Structure of the frequency response masking filter.

fixed FIR filters, more specifically, i.e., the frequency response masking technique and its extension—the fast filter bank. Section III defines the variable bandedge filter specifications. The principle and structure of the proposed variable filter are presented in Section IV. Section V gives a detailed analysis on the determination of the parameters of each building block in constructing the variable filter. An implementation issue regarding the realization of the modulation is discussed in Section VI. In Section VII, the computational and implementation complexities, as well as the passband-edge variation range, of the variable filter are analyzed and compared. A design example is given in Section VIII to show the efficiency of the proposed technique.

II. Frequency Response Masking Technique and Fast Filter Bank

A very efficient technique to design fixed sharp FIR filters with low complexity is frequency response masking (FRM) [17]–[20]. The variable filter design proposed in this paper is making use of the FRM and its extension—the fast filter bank (FFB) [21]. This section reviews these two techniques.

Just as the name implies, FRM uses masking filters to obtain the desired frequency responses. The structure of the FRM is shown in Fig. 1. Every delay of a bandedge shaping prototype filter, $F(e^{j\omega})$, is replaced by L delays. The frequency response of the resulting filter, $F(e^{jL\omega})$, is a frequency compressed (by a factor of L) version of that of $F(e^{j\omega})$, where the transition band of $F(e^{j\omega})$ is mapped to L transition bands with transition width shrunk by a factor of L, as shown in Fig. 2(a) and (b). The complementary filter of $F(e^{jL\omega})$ is obtained by subtracting $F(e^{jL\omega})$ from a pure delay term, $e^{-jLN_F\omega}$, where N_F is the group delay of $F(e^{j\omega})$. Thus, the entire frequency region from dc to Nyquist frequency is decomposed into L bands; $F(e^{jL\omega})$ and its complement hold alternate band respectively. Using two masking filters $G_1(e^{j\omega})$ and $G_2(e^{j\omega})$, as shown in Fig. 2(c), to filter the outputs of $F(e^{jL\omega})$ and its complement, the desired frequency bands are kept and then combined to obtain the final frequency response, shown in Fig. 2(d). The resulting filter has very sharp transition width but very low complexity. Further details on FRM may be found in [17].

An extension of the above technique produces the FFB. The FFB has good frequency selectivity with very low computational complexity. An N-channel analysis FFB decomposes the input signal into N channels in the frequency range from dc to sampling frequency, where N is an integer power of two. Let $N = 2^P$, where P is an integer. The N-channel FFB consists of P levels of filters. The structure of an example of an eight-channel analysis FFB is shown in Fig. 3.

In Fig. 3, the pth level filter $H_a^{p,q}(e^{j\omega})$, for $p = 0, 1, \ldots, P-1$, is a frequency compressed and shifted version of a prototype

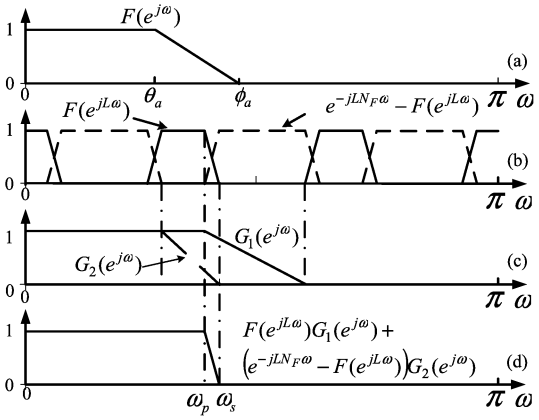

Fig. 2. Frequency responses of FRM sub-filters.

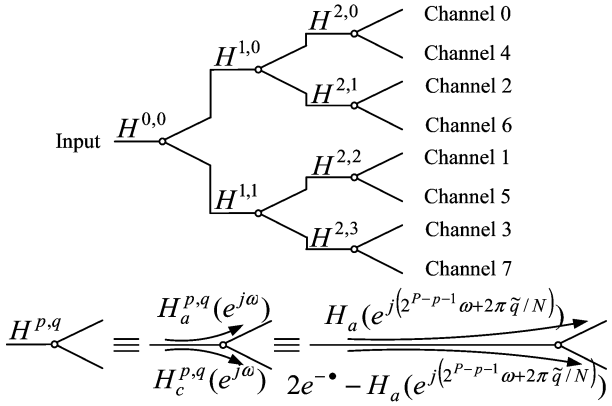

Fig. 3. Structure of an eight-channel analysis FFB. $e^{-\bullet}$ is a delay term of $e^{-jN_{H_a^p}2^{P-p-1}\omega}$.

lowpass half band filter $H_a^p(e^{j\omega})$, of which the passband gain is 2. $H_a^{p,q}(e^{j\omega})$ can be expressed as

$$H_a^{p,q}(e^{j\omega}) = H_a^p(e^{j(2^{P-p-1}\omega+2\pi\widetilde{q}/N)}) \tag{1}$$

where, $\widetilde{q}$ is the bit reversed version of q in $P-1$ bits. In other words, $H_a^{p,q}(e^{j\omega})$ is obtained by replacing each delay of $H_a^p(e^{j\omega})$ by 2^{P-p-1} delays, and then shifting the frequency by $2\pi\widetilde{q}/(2^{P-p-1}N)$.

The complimentary filter $H_c^{p,q}(e^{j\omega})$ is related to $H_a^{p,q}(e^{j\omega})$ by

$$H_c^{p,q}(e^{j\omega}) = 2e^{-\bullet} - H_a^{p,q}(e^{j\omega}) \tag{2}$$

where, $e^{-\bullet}$ is a delay term of $e^{-jN_{H_a^p}2^{P-p-1}\omega}$; $N_{H_a^p}$ is the group delay of $H_a^p(e^{j\omega})$.

$H_a^{0,0}(e^{j\omega})$ and $H_c^{0,0}(e^{j\omega})$ have complementary frequency responses as shown in Fig. 4(b), whereas the frequency response of the prototype filter $H_a^0(e^{j\omega})$ is shown in Fig. 4(a). The frequency responses of the subsequent levels of prototype filters are compressed by respective factors and then shifted by an appropriate amount if necessary, to mask out the unwanted channels. For example, the cascade of $H_c^{0,0}(e^{j\omega})$, $H_a^{1,1}(e^{j\omega})$ and $H_c^{2,2}(e^{j\omega})$ leads to the output of channel 5. The frequency responses of $H_a^{1,1}(e^{j\omega})$, $H_a^{2,2}(e^{j\omega})$ and their complements are

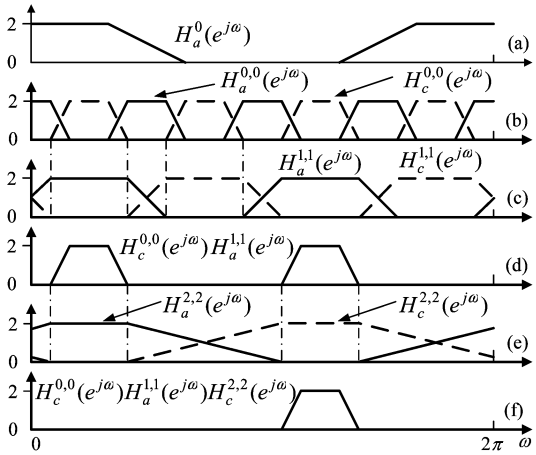

Fig. 4. Frequency responses of filters for deriving channel 5 in an eight-channel FFB.

shown in Fig. 4(c) and (e). The intermediate and final masking results are shown in Fig. 4(d) and (f).

The N-channel ($N = 2^P$) FFB generates uniform filter banks with transition bands centered at $(2n+1)\pi/N$, for $n = 0, 1, \ldots, N-1$. To have the filter banks with transition width of ω_t, the passband edge ϕ_0 of the prototype half band filter $H_a^0(e^{j\omega})$ is set to be $(2\pi - N\omega_t)/4$. The passband edges of the subsequent levels of the prototype filters are chosen as

$$\phi_p = \frac{\pi - \phi_0}{2^p} = \frac{2\pi + N\omega_t}{2^{p+2}} \tag{3}$$

for level $p = 1, 2, \ldots, P-1$.

The FRM and FFB provide efficient ways to design sharp transition band filters and filter banks with very low computational complexity. However, they cannot be directly extended to design variable filters. In the remainder of this paper, a novel approach is proposed to design variable filters by using FRM and FFB.

III. Variable Bandedge Filter

This section defines the specifications of filters considered in this paper. Traditionally, a design technique for lowpass filters can be transformed to design highpass and bandpass/bandstop filters. The technique proposed in this paper can similarly be extended to the design of highpass and bandpass/bandstop filters. In this paper, only lowpass filters are considered.

Consider a lowpass filter with a passband edge of ω_p and transition width of $\Delta\omega$. The maximum passband and stopband ripple magnitudes are δ_p and δ_s, respectively. ω_p is variable in a range of $[\omega_l, \omega_u]$, whereas $\Delta\omega$, δ_p, δ_s, ω_l, and ω_u are fixed for a given design. Thus, the frequency response of the variable filter, $H\left(e^{j\omega}, \omega_p\right)$, satisfies the following constraints:

$$\begin{aligned} 1-\delta_p \le H\left(e^{j\omega}, \omega_p\right) \le 1+\delta_p, \quad \omega \in [0, \omega_p] \\ -\delta_s \le H\left(e^{j\omega}, \omega_p\right) \le \delta_s, \quad \omega \in [\omega_p + \Delta\omega, \pi] \end{aligned} \tag{4}$$

for $\omega_l \le \omega_p \le \omega_u$, $0 \le \omega_l < \omega_u \le \pi - \Delta\omega$, and $\Delta\omega > 0$. The variation range of the passband edge, simply referred to as variation range in the following of the paper, is defined as $\omega_u - \omega_l$. The set of specifications is illustrated in Fig. 5.

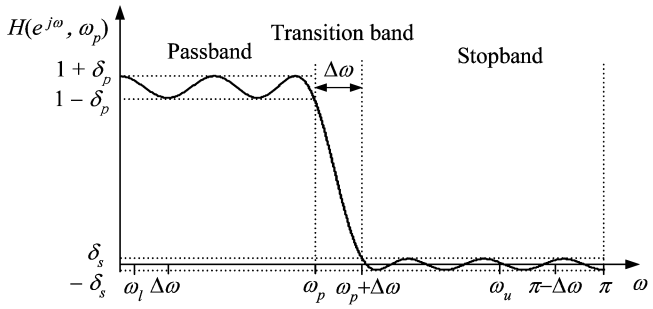

Fig. 5. Specifications for a lowpass filter with variable bandedge frequency.

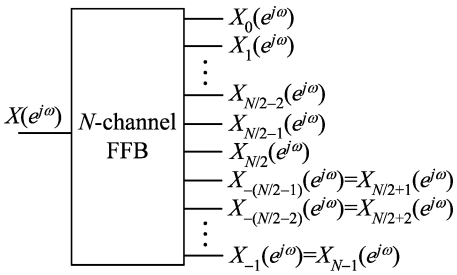

Fig. 6. Symbol of an FFB.

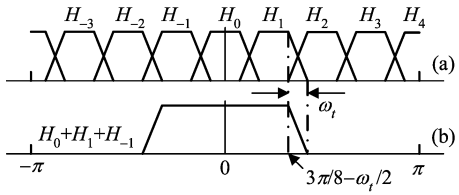

Fig. 7. (a) Eight-channel FFB with transition width ω_t. (b) Frequency response of a discretely tunable filter with bandedge at discrete frequency $(2n+1)\pi/N - \omega_t/2$, for $N = 8$ and $n = 1$.

IV. Principle and Structure of the Proposed Variable Filter

Fig. 6 shows the symbol of an N-channel FFB, where the input signal is decomposed into N channels. For expository convenience, from this section onwards, the N channels in the frequency range $-f_N$ to f_N are considered, where, f_N is the Nyquist frequency. The N channels are re-labeled as 0, ± 1, $\pm 2, \ldots, \pm(N/2-1)$, and $N/2$. The frequency response of the nth channel, represented as $H_n(e^{j\omega})$ for $n = 0, \pm 1, \cdots \pm (N/2-1), N/2$, is shown in Fig. 7(a). [The $e^{j\omega}$ term is omitted in Figs. 7, 8(b) and 10(a).] For an input signal with spectrum $X(e^{j\omega})$ as shown in Fig. 6, the output for channel n is denoted as $X_n(e^{j\omega})$, for $n = 0, \pm 1, \ldots, \pm(N/2-1)$, and $N/2$. For real input, the output $X_0(e^{j\omega})$ and $X_{N/2}(e^{j\omega})$ are real, whereas $X_n(e^{j\omega})$ for $n = \pm 1, \cdots, \pm(N/2-1)$ is complex. Furthermore, $X_n(e^{j\omega})$ is the complex conjugate of $X_{-n}(e^{j\omega})$, for $n = 1, 2, \ldots, N/2-1$. Therefore, summing $X_n(e^{j\omega})$ and $X_{-n}(e^{j\omega})$ results in a real output. The same effect can be achieved by taking the real part of $X_n(e^{j\omega})$ and then scaling it by a factor of 2.

A. Discretely Tunable Filter

From Fig. 7(a), it can been seen that FFB can serve as a variable bandedge filter by combining the proper channels; the re-

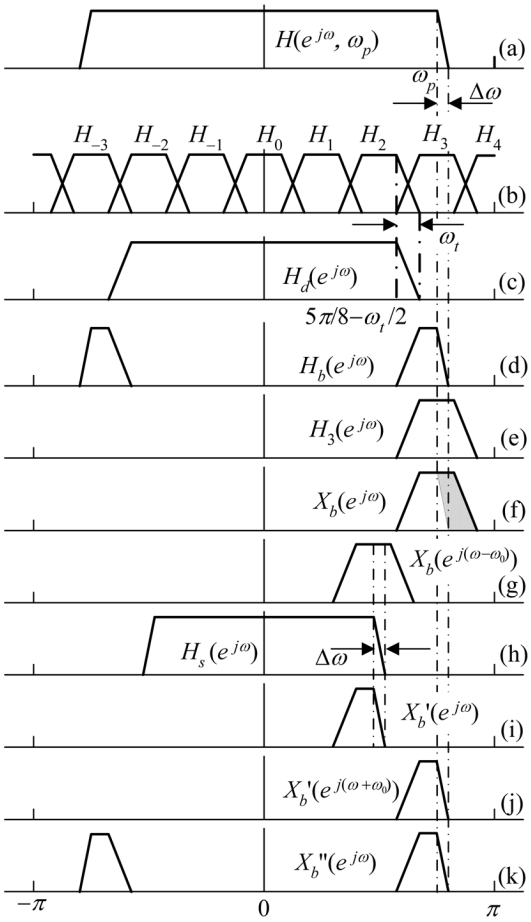

Fig. 8. Frequency responses and signal frequency spectrums in the course of generating the continuously tunable filters.

sulting variable filter, however, has bandedges only at a set of discrete frequency values. For example, an N-channel FFB with transition width ω_t may generate lowpass filter with passband edge at $(2n+1)\pi/N - \omega_t/2$ for $n = 0, 1, \ldots, N/2-1$ by combining channels from channel 0 to channel $(\pm n)$. Fig. 7(b) shows one of the variation of a lowpass filter with transition width ω_t synthesized from an eight-channel FFB. By combining channels 0 and ± 1, the resulting lowpass filter has passband edge at $3\pi/8 - \omega_t/2$. The bandedge of a filter synthesized by combining the outputs of an FFB can be adjusted only in discrete step; such a filter is called a discretely tunable filter.

B. Continuously Tunable Filter

An example is used to illustrate the principle of the design of continuously tunable filter.

Suppose that it is desired to design a lowpass filter with frequency response $H\left(e^{j\omega}, \omega_p\right)$, as shown in Fig. 8(a), where ω_p is the passband edge; the transition width of the lowpass filter $H\left(e^{j\omega}, \omega_p\right)$ is $\Delta\omega$. Suppose also that an eight-channel FFB is adopted, and ω_p is not located at any of the discrete values $(2n+1)\pi/N - \omega_t/2$ for $N = 8$, and $n = 0, 1, 2, 3$. The filter synthesis process goes as follows.

First, a discrete tunable filter is synthesized by combining channels 0, ± 1 and ± 2 to have the discrete stopband edge smaller than $\omega_p + Dw$. The frequency response of the discrete bandedge filter, denoted as $H_d(e^{j\omega})$, is shown in Fig. 8(c). Let the output of $H_d(e^{j\omega})$ be $X_d(e^{j\omega})$.

Second, we attempt to synthesize a bandpass filter having frequency response $H_b(e^{j\omega})$ as shown in Fig. 8(d) in such a way that the combination of $H_d(e^{j\omega})$ and $H_b(e^{j\omega})$ produces the desired lowpass response.

Last, the output of the discretely tunable filter $H_d(e^{j\omega})$ is then added to the output of the bandpass filter $H_b(e^{j\omega})$ to form the desired output of the continuously tunable lowpass filter.

The bandpass filter $H_b(e^{j\omega})$ proposed in the second step may be obtained as follows.

1) A bandpass channel is selected from the FFB. In this example, channel 3 with frequency response $H_3(e^{j\omega})$ as shown in Fig. 8(e) is selected. In case the transition band of the variable filter in a given variation is located in the transition bands of the FFB channels, the two adjacent bandpass channels are selected and combined. The detailed approach to selecting the bandpass channel(s) is given in Section IV-C. Let the output of the selected bandpass channel(s), i.e., $H_3(e^{j\omega})$ in this example, be $X_b(e^{j\omega})$, as shown in Fig. 8(f).
2) $X_b(e^{j\omega})$ is shifted in the frequency domain by an appropriate amount ω_0 to become $X_b(e^{j(\omega-\omega_0)})$, as shown in Fig. 8(g).
3) $X_b(e^{j(\omega-\omega_0)})$ is then filtered by a lowpass filter whose frequency response, $H_s(e^{j\omega})$, is shown in Fig. 8(h), to produce the output signal $X_b'(e^{j\omega}) = X_b(e^{j(\omega-\omega_0)})H_s(e^{j\omega})$ shown in Fig. 8(i). This lowpass filter $H_s(e^{j\omega})$ is a fixed filter with the same transition width, $\Delta\omega$, as that of $H\left(e^{j\omega}, \omega_p\right)$. $H_s(e^{j\omega})$ is referred to as bandpass shaping filter. The purpose of shifting $X_b(e^{j\omega})$ in the frequency domain and using the bandpass shaping filter is to remove the frequency component in $X_b(e^{j\omega})$ corresponding to the stopband of $H\left(e^{j\omega}, \omega_p\right)$. The frequency component in $X_b(e^{j\omega})$ to be removed is shown as the shaded region in Fig. 8(f).
4) $X_b'(e^{j\omega})$ is then shifted back to its original frequency location to form $X_b'(e^{j(\omega+\omega_0)})$ as shown in Fig. 8(j).
5) $X_b'(e^{j(\omega+\omega_0)})$ is complex. The desired output of the bandpass filter $H_b(e^{j\omega})$ is obtained as twice the real part of $X_b'(e^{j(\omega+\omega_0)})$. The spectrum of the desired output of the bandpass filter denoted as $X_b''(e^{j\omega})$ is shown in Fig. 8(k).

The block diagram of the bandpass filter $H_b(e^{j\omega})$ is shown in Fig. 9.

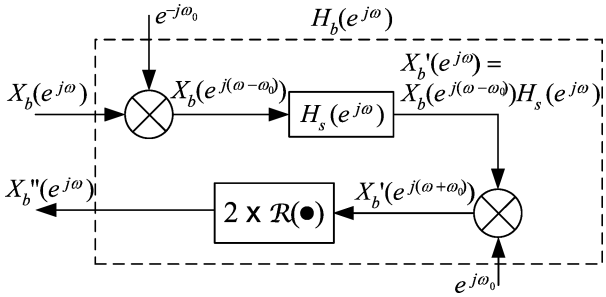

Fig. 9. Bandpass filter $H_b(e^{j\omega})$, where $\Re(\bullet)$ = real part of $\bullet$.

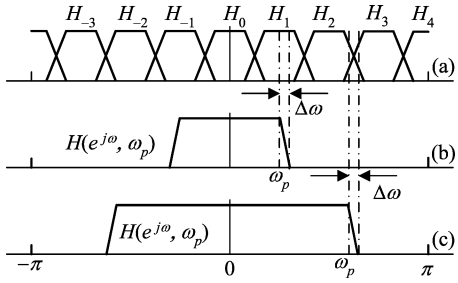

Fig. 10. Illustration of the transition band location of the variable filter with respect to the FFB channels. (a) Frequency response of an eight-channel FFB. (b) Transition band of the variable filter is located within the passband of a single FFB channel, and (c) Transition band of the variable filter is located at the junction of two FFB channels.

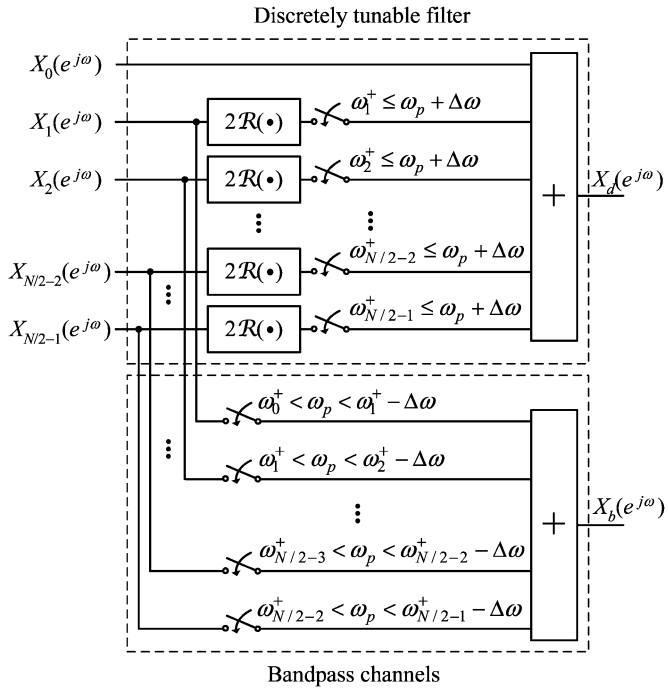

Fig. 11. Block diagram of channel selector for the construction of the discrete tunable filter and bandpass filter, where $\omega_n^- = (2n+1)\pi/N - \omega_t/2$, and $\omega_n^+ = (2n+1)\pi/N + \omega_t/2$. The switch is on when the condition on the side of the switch is satisfied.

C. Channel Selection for the Construction of Continuously Tunable Filter

For any given ω_p, the channels used to construct the discretely tunable filter $H_d(e^{j\omega})$ and the bandpass filter $H_b(e^{j\omega})$ must be determined.

To construct the continuously tunable filter using the technique described in Section IV-B, the stopband edge of the discretely tunable filter must not be larger than $\omega_p+\Delta\omega$, but closest to $\omega_p+\Delta\omega$. $\omega_p+\Delta\omega$ is the stopband edge of the desired variable lowpass filter, $H\left(e^{j\omega}, \omega_p\right)$. The discretely tunable filter consists of channel $(\pm n)$ of the FFB where n satisfies the constraint

$$\frac{(2|n|+1)\pi}{N} + \frac{\omega_t}{2} \le \omega_p + \Delta\omega, \text{ for } 0 < |n| < \frac{N}{2}. \quad (5)$$

Note that channel 0 is always selected for the construction of the discretely tunable filter. As a consequence, the minimum band of the variable filter that can be synthesized is that of channel 0.

In generating the output of the discretely tunable filter, besides the output of channel 0, conjugate output of channel pairs of $\pm n$ for n satisfying (5) are summed together. As the same effect of such summation can be achieved by taking the real part of the output of channel n, and scaling it by a factor of 2, in actual implementation, channel n is used, while channel $(-n)$ is ignored, as shown in Fig. 11.

In the selection of bandpass channels for the construction of the bandpass filter, there are two cases. In the first case, the transition band of $H\left(e^{j\omega}, \omega_p\right)$ is located entirely in the passband of a single channel of FFB, for example, the variation of ω_p shown in Fig. 10(b). The transition band of the variable filter is located inside channel 1. Channel 1 is thus selected for the construction of the bandpass filter. In the second case, the transition band of $H\left(e^{j\omega}, \omega_p\right)$ is located at the junction of two channels, as shown in Fig. 10(c); in this case, both channels, (channels 2 and 3 in the example of Fig. 10(c)), are selected and their outputs are summed to construct the bandpass filter. Considering the above two cases, channel n is selected for the construction of the bandpass filter if

$$\frac{(2n-1)\pi}{N} - \frac{\omega_t}{2} < \omega_p < \frac{(2n+1)\pi}{N} + \frac{\omega_t}{2} - \Delta\omega, \quad \text{for } 0 < n < \frac{N}{2}, \quad (6)$$

is satisfied. Note that channel $(N/2)$ is not selected to construct the bandpass filter in any case. As a consequence, the maximum band of the variable filter that can be synthesized is not larger than the combination of channels from 0 to $\pm(N/2-1)$.

Based on (5) and (6), the diagram of the channel selector for the construction of the discrete tunable filter and bandpass filter is illustrated in Fig. 11.

The overall structure of the variable filter, consisting of an FFB, a channel selector and a bandpass filter, is shown in Fig. 12, where the channel selector block is shown in Fig. 11, and the bandpass filter block is shown in Fig. 9.

V. Specifications for the FFB and the Bandpass Shaping Filter

The determination of the various parameters of the FFB and the bandpass shaping filter are discussed in this section.

A. Bandpass Shaping Filter $H_s(e^{j\omega})$

The function of the bandpass shaping filter is to remove the frequency component of $X_b(e^{j\omega})$, the output of the selected bandpass channels, that corresponds to the stopband of the variable filter. $H_s(e^{j\omega})$ is thus required to have a transition band width of $\Delta\omega$. Furthermore, depending on the location of the variable bandedge ω_p, it is equally possible for $H_s(e^{j\omega})$ to retain or to remove the majority of the frequency component of $X_b(e^{j\omega})$. This implies that both the passband and stopband width of $H_s(e^{j\omega})$ must be as wide as the spectrum width of

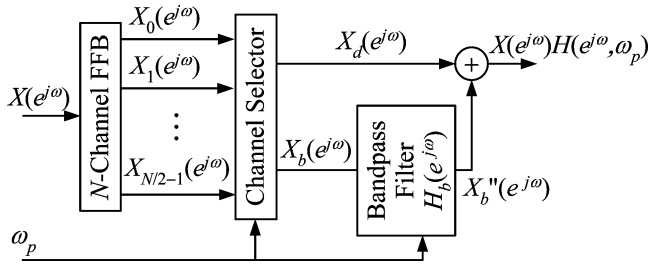

Fig. 12. Overall structure of the variable filter.

$X_b(e^{j\omega})$. Therefore, it is reasonable to design the bandpass shaping filter to have the same passband and stopband width.

Due to the above consideration, a half band filter with transition width $\Delta\omega$ is adopted as the passband shaping filter to reduce the computational complexity.

Thus, the passband edge of the bandpass shaping filter is at $(\pi - \Delta\omega)/2$. The variable bandedge ω_p is aligned with $(\pi - \Delta\omega)/2$ after it is shifted by ω_0 along with the shifting of the output of the selected bandpass channels $(X_b(e^{j\omega}))$. Therefore, $X_b(e^{j\omega})$ is to be shifted by $\omega_0 = (\pi - \Delta\omega)/2 - \omega_p$ in the frequency domain.

B. Number of Channels of the FFB

Before a detailed computational complexity analysis of an N-channel FFB is presented in Section VII, it is obvious from the structure of the FFB that the computational complexity of the FFB increases with increasing N. To keep the overall computational complexity low, the number of channels of the FFB should be as few as possible, subject to the condition that the performance of the variable filter is not affected.

In the construction of the bandpass filter $H_b(e^{j\omega})$, either a single channel or two adjacent channels are selected, as shown in Section IV-C, depending on the location of the variable bandedge. When $N = 8$, the frequency range occupied by the combination of two channels is wider than the passband of the bandpass shaping filter in the positive frequency range, as the bandpass shaping filter is a half band filter. In such a case, aliasing may be produced in the cause of bandpass shaping. Therefore, a good choice of N is 16, which corresponds to $P = 4$.

C. Ripples of the Prototype Filters of the FFB and of the Bandpass Shaping Filter

The prototype filters used to construct the FFB are half band filters, as described in Section II. Half band filters have the same maximum ripple in the passband and stopband. Therefore, every prototype filter of the FFB, as well as the bandpass shaping filter, has equal maximum passband and stopband ripples. To simplify the analysis, we assume that all the prototype filters of FFB and the bandpass shaping filter have the same maximum ripple, δ. Since the channels are generated using complementary filters, and the combination of all channels is an idea all-pass filter, for a P level ($N = 2^P$ channel) FFB, the worst case ripple magnitude is $P\delta$ in both the passband and stopband, irrespective of the number of channels being combined. The bandpass shaping filter may introduce additional δ ripple for the final output, i.e., the overall ripple magnitude of the variable filter in the worst case is $(P + 1)\delta$.

Thus, to design the variable filter having passband and stopband ripple of δ_p and δ_s, the worst case ripple allowed for each prototype filter and the bandpass shaping filter is

$$\delta_w = \frac{\min(\delta_p, \delta_s)}{P+1}. \tag{7}$$

However, the ripples of the cascaded filters may cancel each other. From our experience, the ripple magnitude of the prototype filters and the bandpass shaping filter may be relaxed to

$$\delta = 2.5\delta_w. \tag{8}$$

The resulting variable filter, in general, still meets the given specification. When P is selected to be 4 as suggested in Section V-B, according to (7), (8) is simplified to

$$\delta = 2.5 \times \frac{\min(\delta_p, \delta_s)}{4+1} = \frac{\min(\delta_p, \delta_s)}{2}. \tag{9}$$

D. Bandedge of the Prototype Filter $H_a^0(e^{j\omega})$

Since the transition band of the variable filter is determined by the bandpass shaping filter $H_s(e^{j\omega})$, the bandedge of the prototype filter $H_a^0(e^{j\omega})$ can have arbitrary value between 0 and $\pi/2$. It has been shown in Section II that the bandedge of $H_a^0(e^{j\omega})$, ϕ_0, determines the bandedges of all other level prototype filters. Thus, ϕ_0 is chosen in such a manner that the overall computational complexity of the FFB is minimized. The number of nontrivial coefficients of a half band filter, with ripple δ and normalized transition width of β, is approximately given by $\Phi_H(\delta)/\beta + 1 \approx \Phi_H(\delta)/\beta$, (thus, the order of the half band filter is approximately $2\Phi_H(\delta)/\beta$), where $\Phi_H(\delta)$ is given by [22]

$$\Phi_H(\delta) = 0.002655\log_{10}^3\delta + 0.03424\log_{10}^2\delta - 0.5351\log_{10}\delta - 0.2139. \tag{10}$$

Based on the prototype filter $H_a^p(e^{j\omega})$, 2^p filters are generated for level p. Among these filters, there are three types of filters in view of the computational complexity: type A filter has real filter coefficients and real input signal, type B has complex filter coefficients and real input signal, whereas both filter coefficients and input signal are complex for type C filter. To generate one sample output, the number of multiplications for filters of type A, B, and C are once, twice and four times of the number of the nontrivial coefficients, respectively. Except that level 0 has only 1 type A filter, all other levels have 1 type A filter, 1 type B filter, and $2^p - 2$ type C filters, for level p. Thus, the overall number of multiplications to compute one output sample for all channels from channel 0 to channel $(N/2 - 1)$ is given by

$$C_b = \frac{\Phi_H(\delta)}{\beta_0} + \sum_{p=1}^{P-1} \frac{[1 + 2 + 4(2^p - 2)]\Phi_H(\delta)}{\beta_p}. \tag{11}$$

TABLE I
BEST CHOICES OF ϕ_0 AND THE CORRESPONDING COMPUTATIONAL COMPLEXITY, C_b, FOR A 2^P-CHANNEL FFB

P	ϕ_0	C_b
4	0.389π	$119.8\Phi_H(\delta)$, where $\delta = \min(\delta_p, \delta_s)/2$
5	0.398π	$237.5\Phi_H(\delta)$, where $\delta = 5 \times \min(\delta_p, \delta_s)/12$
6	0.405π	$503.1\Phi_H(\delta)$, where $\delta = 5 \times \min(\delta_p, \delta_s)/14$

Substituting β_p, the normalized transition width of the pth level prototype filter, by $(\pi - 2\phi_p)/(2\pi)$, where ϕ_p for $p = 1, \ldots, P-1$ is given by (3), we have

$$C_b = \frac{\Phi_H(\delta)\cdot 2\pi}{\pi - 2\phi_0} + \sum_{p=1}^{P-1} \frac{(2^{p+2}-5)\Phi_H(\delta)\cdot 2\pi}{\pi - 2\phi_p} = \frac{\Phi_H(\delta)\cdot 2\pi}{\pi - 2\phi_0} + \sum_{p=1}^{P-1} \frac{(2^{p+2}-5)\Phi_H(\delta)\cdot 2\pi}{\pi - \frac{2(\pi-\phi_0)}{2^p}} \quad (12)$$

where $P = \log_2 N$.

The best choices of ϕ_0 and the corresponding C_b for $P = 4, 5$, and 6, which corresponds to 16-, 64-, and 128-channel FFB, are listed in Table I. The values for $P = 5$ and 6 are listed to verify that the computational complexity increases with increasing N.

With the channel number N and ϕ_0, the variation range of the variable filter is determined. It is noticed from the variable filter structure proposed in Section IV, that channel 0 is always combined into the discretely tunable filter, such that the variable passband edge is always not smaller than $2(\pi - \phi_0)/N - \Delta\omega$, i.e., $\omega_l = 2(\pi - \phi_0)/N - \Delta\omega$. Meanwhile, channel $(N/2)$ does not contribute to the passband of the variable filter in any case. Thus, the upper bound of the variable passband edge $\omega_u = [(N-2)\pi + 2\phi_0]/N$. For $N = 16$, this covers a very large range of variation in the range from $0.076\pi - \Delta\omega$ to 0.924π.

It is possible to increase the variation range even further by increasing the number of channels. However, doubling the number of FFB channels results in more than doubling in the computational complexity of FFB as shown in Table I.

E. Design of the Bandpass Shaping Filter

The transition band of the variable filter is shaped by the bandpass shaping filter, which is designed to be a half band filter. Therefore, the passband edge of the bandpass shaping filter is $\pi/2 - \Delta\omega/2$. According to the analysis in Section V-C, the allowed maximum ripple, δ, is set $2.5\delta_w$. Thus, the specification of the bandpass shaping filter is fixed.

To implement the bandpass shaping filter with low complexity, the FRM technique for the design of half band filter [23]–[25] is used when the transition band is sharp.

The compression factor L_s in the half band FRM design is chosen to be

$$L_s = \sqrt{\frac{\Phi_H(\delta)}{[\Phi_H(\delta) + \Phi_M(\delta)]\beta}} \quad (13)$$

where β is the normalized transition width $\Delta\omega/(2\pi)$, $\Phi_H(\delta)$ is given in (10), and

$$\Phi_M(\delta) = -0.73294 \log_{10} \delta. \quad (14)$$

Detailed analysis and the optimum order of each subfilter are provided in [25]. The overall complexity of the bandpass shaping filter in terms of the number of multiplications is approximately [25]

$$C_s = 4\sqrt{\frac{[\Phi_H(\delta) + \Phi_M(\delta)]\Phi_H(\delta)}{\beta}} \quad (15)$$

where a factor of 2 has been embedded in (15), since the bandpass shaping filter is a type B filter. Equation (15) can be approximated by [25]

$$C_s = 4\sqrt{\frac{2.32}{\beta}}\Phi_H(\delta) \quad (16)$$

when β is smaller than 0.108.

VI. IMPLEMENTATION OF e^{jx} FUNCTION

In the proposed variable filter technique, $X_b(e^{j\omega})$, the output of the selected bandpass channel(s) is shifted by a frequency of $\pm\omega_0$. The implementation of the frequency shifting in time domain is to modulate the output signal, denoted as $x_b(n)$ in time domain, by $e^{\pm j\omega_0 n} = \cos(\omega_0 n) \pm j\sin(\omega_0 n)$. So, the problem basically is to implement the functions of $\sin(x)$ and $\cos(x)$.

Standard method for obtaining the sine function and cosine function values are table lookup and series expansion. To achieve high frequency resolution with low computational complexity and storage requirement, an efficient implementation makes use of angular decomposition, where the phase angle is expressed as a sum of coarse and fine angles.

Eight multiplications are required to compute $\sin(x)$ and $\cos(x)$ if the angle is computed by the sum of three terms. The corresponding storage required is three $2^{Q/3}$ words of memory blocks, when the angle is represented with a precision of Q bits. A good review for alternative techniques may be found in [26].

Once the sine and cosine values of $-\omega_0 n$ are obtained, $x_b(n)$, a complex signal, is modulated by $e^{j\omega_0 n}$ using four multiplications. The modulated signal is filtered by the bandpass shaping filter, and the resulting output is demodulated by $e^{j\omega_0 n}$ using 4 multiplications again. The value of $e^{j\omega_0 n}$ may be derived in a straightforward manner from that of $e^{-j\omega_0 n}$, since $e^{j\omega_0 n}$ is the complex conjugate of $e^{-j\omega_0 n}$.

Thus, in total, 16 multiplications are required for the modulation and demodulation processes, if the sine and cosine values of any angle are computed by the sum of 3 terms.

VII. COMPLEXITY ANALYSIS

In this section, the complexity of the proposed technique, in terms of computational complexity and implementation complexity is analyzed and compared with other variable digital filters.

A. Computational Complexity

In the operation of the proposed variable filters, multiplications dominate the computational complexity. In this analysis,

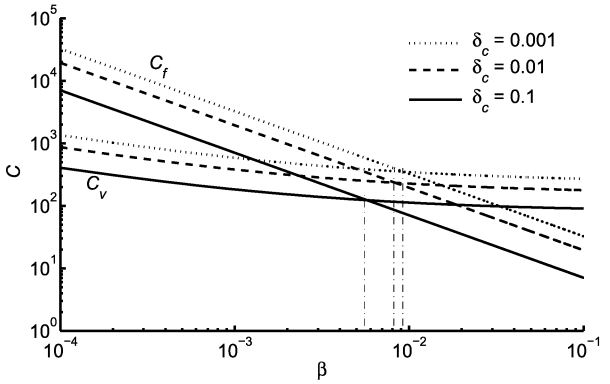

Fig. 13. Comparison of computational complexity of variable filter (C_v) to that of the corresponding fixed filters (C_f) with the same normalized transition width β and passband and stopband ripple δ_c.

the computational complexity is measured in the number of multiplications required to generate one output sample.

From the analysis in Sections V and VI, it is obvious that the overall computational complexity C_v, for a variable filter with normalized transition width β and ripple magnitudes δ_p and δ_s, is given by

$$C_v = C_b + C_s + C_e = 119.8\Phi_H\left(\frac{\delta_c}{2}\right) + 4\sqrt{\frac{2.32}{\beta}}\Phi_H\left(\frac{\delta_c}{2}\right) + 16 \quad (17)$$

for $P = 4$, where $\delta_c = \min(\delta_p, \delta_s)$. C_b is the computational complexity of FFB to separate the signals into 16 channels, C_s is that of bandpass shaping filter, and C_e is that of modulation and demodulation of $x_b(n)$. For a given ripple specification, C_b is independent of the transition width of the variable filter. Therefore, when the transition width of the variable filter is small, the computational complexity for the FFB remains unchanged.

Consider a fixed filter with the normalized transition width β, and ripple $\delta_c = \min(\delta_p, \delta_s)$ in both passband and stopband. The passband and stopband ripple magnitudes are assumed to be the same to simplify the discussion. The computational complexity of the fixed filter, denoted as C_f, is given by

$$C_f = \frac{2\Phi_H(\delta_c)}{\beta}. \quad (18)$$

From (10), (17), and (18), it can be seen that the increase of C_v due to the decrease of β is slower than that of C_f, since C_v is proportional to $\sqrt{1/\beta}$, whereas C_f is proportional to $1/\beta$.

The plots of the curves of C_f and C_v versus β for typical values of $\delta_c = 0.1$, 0.01 and 0.001 are shown in Fig. 13.

It can be seen from Fig. 13 that when β is smaller than 0.0057, 0.0083, and 0.0093, for $\delta_c = 0.1$, 0.01 and 0.001, respectively, the computational complexity of the variable filter is even lower than its corresponding fixed filters with the same β and δ_c.

B. Implementation Complexity

The implementation complexity of the computational elements is consistent with the computational complexity, i.e., the number of multipliers to be implemented is the same as the number of multiplications to generate one output sample. Besides the computational elements, the non-computational components used in the proposed technique includes digital comparators, delay elements and memory block. The required memory block size in the proposed algorithm has been analyzed in Section VI. In this subsection, the implementation complexity in terms of the number of digital comparators and delay elements is discussed.

1) Digital Comparator: Digital comparators are used to control the switches in the channel selector, as shown in Fig. 11. In an N-channel FFB synthesis, the required numbers of switches and comparators are both $N - 2$. While switches could be synthesized using transmission gates, the implementation complexity of a comparator is comparable to (and generally is less than) that of an adder with the same bit width. An adder could directly serve as a digital comparator, since the sign of the sum of one operand and the negative value of the other operand is the result of the comparison. When the difference of the two operands are not required, as in the current case, simpler components could be used. Compared with the implementation complexity of the computational elements, the implementation overhead due to the digital comparators is negligible.

2) Delay Element: To synthesize the FFB, each delay element in the prototype filter in level p is replaced by $2^P - p - 1$ elements. Meanwhile, in the bandpass shaping filter, the half band filter is realized in FRM technique, where each delay in the bandedge shaping filter is replaced by L_s delays. L_s is given in (13). Following the same analysis as in Section V, it is obtained that the total number of delay elements in the proposed technique is approximately

$$D_v = 260.9\Phi_H\left(\frac{\delta_c}{2}\right) + \left(\frac{2}{\beta} + 2\sqrt{\frac{2.32}{\beta}}\right)\Phi_H\left(\frac{\delta_c}{2}\right) \quad (19)$$

when $P = 4$. This value generally is higher than the number of delay elements required in a fixed filter with the same transition width and ripples.

C. Variation Range

The variation range, $\omega_u - \omega_l$, of the proposed technique is determined by the number of FFB channels used in the realization, as discussed in Section V-D. The variation range may be increased at the cost of increasing complexity. The plots of variation range versus estimated computational and implementation complexities for variable filters with $\delta_p = 0.01$, $\delta_s = 0.001$ and $\Delta\omega = 0.01\pi$ synthesized in the proposed technique are shown in Figs. 14 and 15, respectively. The estimated complexities for the technique reported in [16] are also plotted for comparison.

Fig. 14 shows that the computational complexity of the proposed technique is much lower than that reported in [16] when the variation range is not greater than 0.858π. Beyond that, the computational complexity of the proposed technique increases in a piecewise constant mode, but still lower than that of [16] until 0.935π. The computational complexity of the proposed technique exceeds that of [16] in extreme cases where the variation range is larger than 0.935π.

In the synthesis of the variable filters, the proposed technique uses more delay elements, whereas the technique reported in [16] requires a large memory size to store the coefficient values, as shown in Fig. 15. The number of words of memory plotted in

TABLE II
COMPUTATIONAL AND IMPLEMENTATION COMPLEXITY COMPARISON FOR THE FILTER WITH $\Delta\omega = 0.01\pi$, $\delta_p = 0.01$, $\delta_s = 0.001$. ω_p IS IN THE RANGE OF $[0.066\pi, 0.924\pi]$ FOR THE VARIABLE FILTERS

	Computational Complexity	Implementation Complexity				Group Delay
		Multipliers	Delay elements	Words of Memory	Comparators	
Proposed	378	378	1,380	192	14	579
Technique in [16]	1,024	1,024	1,023	86,955	170	507.5
Technique in [10]	$>> 2,160$	$>> 2,160$	$>> 2,160$	0	0	> 270
Fixed filter	510	510	509	0	0	254.5

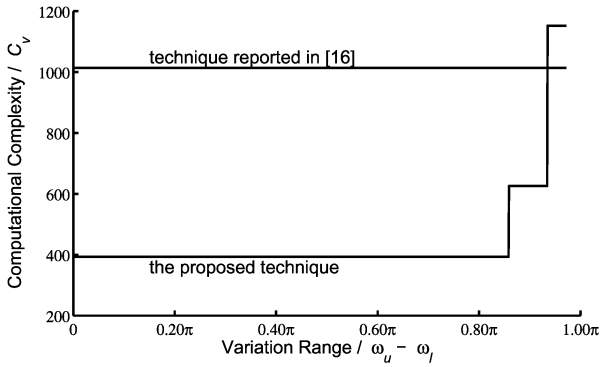

Fig. 14. Computational complexity (C_v) versus variation range for variable filters with $\delta_p = 0.01$, $\delta_s = 0.001$ and $\Delta\omega = 0.01\pi$.

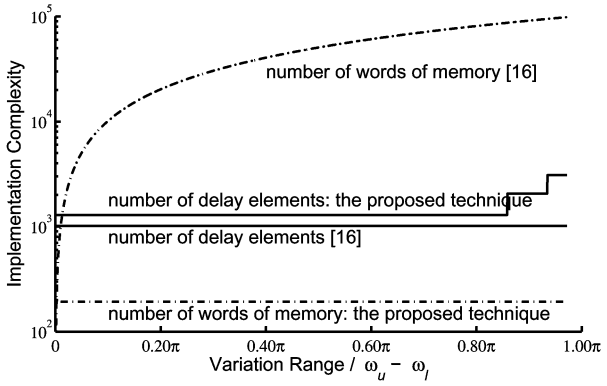

Fig. 15. Implementation complexity versus variation range for variable filters with $\delta_p = 0.01$, $\delta_s = 0.001$ and $\Delta\omega = 0.01\pi$.

Fig. 15 for the proposed technique is obtained assuming that the word length (Q) of the phase angle in the sine and cosine value lookup table is 18. The same assumption is used in Table II.

Another popular technique that is commonly used is the Farrow structure [10], which is notorious for its high computational, implementation and optimization complexity, especially for very sharp transition band filter design. Since the technique proposed in [10] uses a trial and error method to determine the number of filters and filter orders, it is not able to get an estimation of the filter complexities over a wide variation range. To have a sense of the complexity of the technique reported in [10], a small variation range of 0.005π (more specifically, ω_p varying within the range from 0.4975π to 0.5025π) is designed, while the other specifications remain at $\delta_p = 0.01$, $\delta_s = 0.001$ and $\Delta\omega = 0.01\pi$. A linear programming with more than 1,000 unknown variables and about 20,000 constraints is solved. The optimization algorithm runs over 3 hours on a PC with a 3-GHz CPU. The resulting design requires 2160 multipliers and 2156 delay elements. This example shows the extremely high computational, implementation and optimization complexity of the Farrow structure even for such a small variation range. Increasing the variation range requires more and higher order filters in the Farrow structure, if they could ever be optimized.

VIII. NUMERICAL EXAMPLE

A variable filter with the specifications of $\Delta\omega = 0.01\pi$, $\delta_p = 0.01$ and $\delta_s = 0.001$ is designed.

According to the analysis in Section V, a 16-channel FFB is adopted. Thus, the passband edge of the variable filter may vary in the range from 0.066π to 0.924π. The passband edge ϕ_0 of the prototype filter $H_a^0(e^{j\omega})$ is chosen to be 0.389π, and the passband edges ϕ_p of the subsequent level prototype filters $H_a^p(e^{j\omega})$, for $p = 1,2,3$ are 0.3055π, 0.1528π and 0.0764π, obtained using (3). The passband and stopband ripples of these filters are set to $\min(\delta_p, \delta_s)/2 = 0.0005$ according to (9). The estimated filter orders and actual filter orders satisfying these bandedge and ripple requirements are 30, 16, 7, 4 and 34, 18, 10, 6, respectively, for $H_a^p(e^{j\omega})$ for $p = 0,1,2,3$. All these filters are half band filters.

The passband edge of the bandpass shaping filter is 0.495π and its ripple magnitude is 0.0005. The compression factor L_s is chosen as 9 according to (13). The filter lengths for the three subfilters $A(e^{j\omega})$, $B(e^{j\omega})$ and $C(e^{j\omega})$ in the FRM structure [23] are 83, 49, and 51, respectively, where filters $A(e^{j\omega})$ and $C(e^{j\omega})$ are half band filters, and filter $B(e^{j\omega})$ consists of terms with only odd power of $e^{j\omega}$.

The total computational complexity is

$$\begin{aligned} C &= C_b + C_s + C_e \\ &= \left(\frac{34}{2} + \frac{18}{2} \times 3 + \frac{10}{2} \times 11 + \frac{6}{2} \times 27\right) \\ &\quad + \left(\frac{83-1}{2} + \frac{49+1}{2} + \frac{51-1}{2}\right) \times 2 + 16 \\ &= 180 + 182 + 16 = 378. \end{aligned} \tag{20}$$

For comparison, a fixed filter with the same $\Delta\omega$, δ_p, and δ_s requires 510 multiplications to implement. This verifies the analysis that the variable filter may have lower computational complexity than its corresponding fixed filter with the same transition width and ripple requirements. The proposed variable filter structure is the first technique that achieves such low computational complexity.

The computational and implementation complexity compared with the fixed filter, as well as the techniques reported in [16] and [10] for this particular example is listed in Table II.

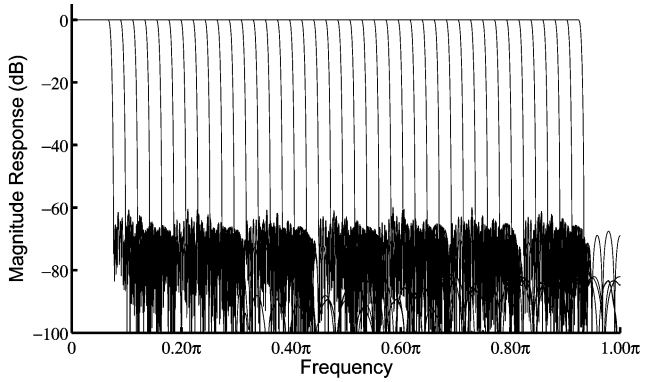

Fig. 16. Magnitude responses of the variable filters for $\Delta\omega = 0.01\pi$, $\delta_p = 0.01$, $\delta_s = 0.001$ and $\omega_p = 0.066\pi, 0.088\pi, 0.110\pi, \ldots, 0.924\pi$.

In Table II, "$\gg$" refers to "much larger than." The values for the technique reported in [10] are estimated based on the design with variation range of 0.005π.

The complexity reduction of the proposed technique in both computation and implementation is attributed to the FRM technique, although directly application of FRM may not achieve the same effect. The price paid for all these savings is the increase in group delay.

In the above, as well as in Section VII, when counting the number of multiplications, the symmetry of the coefficients of all design techniques is not considered. If the symmetry of the coefficients is considered, the numbers of required multiplications are reduced by a factor of two. Note that the symmetry of the coefficients has been considered in calculating the memory size of the technique reported in [16]

The magnitude responses of the variable filter for $\omega_p = 0.066\pi, 0.088\pi, 0.110\pi, \ldots, 0.924\pi$, obtained using the proposed technique, are shown in Fig. 16.

IX. Conclusion

This paper proposed an efficient approach to designing variable bandedge FIR filters with sharp transition band. The variable filter is constructed from a fixed FFB and a fixed half band filter, whereas the variation of the filter is realized by shifting the signals in the frequency domain. Since fixed filters plus FRM technique are used, the proposed technique achieves extremely low computational complexity when the transition band is sharp.

References

[1] W. Schuessler and W. Winkelnkemper, "Variable digital filters," *(AEU) Arch. Elektr. Ubertragung*, vol. 24, pp. 524–525, 1970.

[2] A. V. Oppenheim, W. F. G. Mechlenbräuker, and R. M. Mersereau, "Variable cutoff linear phase digital filters," *IEEE Trans. Circuits Syst.*, vol. 23, pp. 199–203, Apr. 1976.

[3] R. E. Crochiere and L. R. Rabiner, "On the properities of frequency transformations for variable cutoff linear phase digital filters," *IEEE Trans. Circuits Syst.*, vol. 23, pp. 684–686, Nov. 1976.

[4] S. S. Ahuja and S. C. D. Roy, "Linear phase variable digital bandpass filters," *Proc. IEEE*, vol. 67, pp. 173–174, Jan. 1979.

[5] S. C. C. Roy and S. S. Ahuja, "Frequency transformations for linear-phase variable-cutoff digital filters," *IEEE Trans. Circuits Syst.*, vol. CAS-26, pp. 73–75, Jan. 1979.

[6] P. Jarske, Y. Neuvo, and S. K. Mitra, "A simple approach to the design of linear phase FIR digital filters with variable characteristics," *Signal Process. (Elsevier)*, vol. 14, pp. 313–326, 1988.

[7] S. C. Chan, C. K. S. Pun, and K. L. Ho, "A new method for designing FIR filters with variable characteristics," *IEEE Signal Process. Lett.*, vol. 11, pp. 274–277, Feb. 2004.

[8] K. M. Tsui *et al.*, "On the minimax design of passband linear-phase variable digital filters using semidefinite programming," *IEEE Signal Process. Lett.*, vol. 11, pp. 867–870, Nov. 2004.

[9] T. B. Deng, "Weighted least-squares method for designing arbitrarily variable 1-D FIR digital filters," *Signal Process. (Elsevier)*, vol. 4, pp. 597–613, Apr. 2000.

[10] P. Löwenborg and H. Johansson, "Minimax design of adjustable-bandwidth linear-phase FIR filters," *IEEE Trans. Circuits Syst. I*, vol. 53, pp. 431–439, Feb. 2006.

[11] C. W. Farrow, "A continuously variable digital delay element," in *Proc. IEEE ISCAS'88*, Espoo, Finland, Jun. 1988, pp. 2641–2645.

[12] J. Vesma and T. Saramäki, "Optimization and efficient implementation of FIR filters with adjustable factional delay," in *Proc. IEEE ISCAS'97*, Hong Kong, PRC, Jun. 1997, pp. 2256–2259.

[13] H. Johansson and P. Löwenborg, "On the design of adjustable fractional delay FIR filters," *IEEE Trans. Circuits Syst. II*, vol. 50, pp. 164–169, Apr. 2003.

[14] J. Yli-Kaakinen and T. Saramäki, "Mulitplication-free polynomial-based FIR filters with and adjustable fractional delay," *Circuits Syst. Signal Process.*, vol. 25, pp. 265–294, 2006.

[15] T. B. Deng, "Noniterative WLS design of allpass variable fractional-delay digital filters," *IEEE Trans. Circuits Syst. I*, vol. 53, pp. 358–371, Feb. 2006.

[16] H. Johansson and P. Löwenborg, "On linear-phase FIR filters with variable bandwidth," *IEEE Trans. Circuits Syst. II*, vol. 51, pp. 181–184, Apr. 2004.

[17] Y. C. Lim, "Frequency-response masking approach for the synthesis of sharp linear phase digital filters," *IEEE Trans. Circuits Syst.*, vol. 33, pp. 357–364, Apr. 1986.

[18] Y. C. Lim and Y. Lian, "The optimum design of one- and two-dimensional FIR filters using the frequency-response masking technique," *IEEE Trans. Circuits Syst. II*, vol. 40, pp. 88–95, Feb. 1993.

[19] W. S. Lu and T. Hinamoto, "Optimal design of frequency-response masking filters using semidefinite programming," *IEEE Trans. Circuits Syst. I*, vol. 50, pp. 557–568, Apr. 2003.

[20] T. Saramäki, J. Yli-Kaakinen, and H. Johansson, "Optimization of frequency-response-masking based FIR filters," *Circuits, Syst. Signal Process.*, vol. 12, pp. 563–590, Oct. 2003.

[21] Y. C. Lim and B. F. Boroujeny, "Fast filter bank (FFB)," *IEEE Trans. Circuits Syst. II*, vol. 39, pp. 316–318, May 1992.

[22] O. Herrmann, L. R. Rabiner, and D. S. K. Chan, "Practical design rules for optimum finite impulse response low-pass digital filters," *Bell Syst. Tech. J.*, vol. 52, pp. 769–799, Jul.–Aug. 1973.

[23] T. Saramäki, Y. C. Lim, and R. Yang, "The synthesis of half-band filter using frequency-response masking technique," *IEEE Trans. Circuits Syst. II*, vol. 42, pp. 58–60, Jan. 1995.

[24] Y. C. Lim, Y. J. Yu, and T. Saramäki, "Optimum masking levels and coefficient sparseness for Hilbert transformers and half-band filters designed using the frequency-response masking technique," *IEEE Trans. Circuits Syst. I*, vol. 52, pp. 2444–2453, Nov. 2005.

[25] Y. C. Lim and Y. J. Yu, "Synthesis of very sharp hilbert transformer using the frequency-response masking technique," *IEEE Trans. Signal Process.*, vol. 53, pp. 2595–2597, Jul. 2005.

[26] J. M. P. Langlois and D. Al-Khalili, "Phase to sinusoid amplitude conversion techniques for direct digital frequency synthesis," *Proc. Inst. Electr. Eng.—Circuits, Devices, Systems*, vol. 151, pp. 519–528, Dec. 2004.

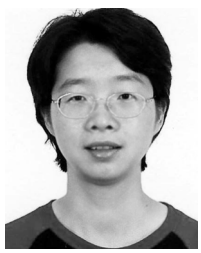

Ya Jun Yu (S'99–M'05) received both the B.Sc. and M.Eng. degrees in biomedical engineering from Zhejiang University, Hangzhou, China, in 1994 and 1997, respectively, and the Ph.D. degree in electrical and computer engineering from the National University of Singapore, Singapore, in 2004.

From 1997 to 1998, she was a Teaching Assistant with Zhejiang University. She joined the Department of Electrical and Computer Engineering, National University of Singapore as a Post Master Fellow in 1998 and remained in the same department as a Research Engineer until 2004. In 2002, she was a Visiting Researcher at the Tampere University of Technology, Tampere, Finland, and the Hong Kong Polytechnic University, Hong Kong, China. She joined the Temasek Laboratories at Nanyang Technological University as a Research Fellow in 2004. Since 2005, she has been with the School of Electrical and Electronic

Engineering, Nanyang Technological University, Singapore, where she is currently an Assistant Professor. Her research interests include digital signal processing and VLSI circuits and systems design.

Yong Ching Lim (S'79–M'82–SM'92–F'00) received the A.C.G.I. and B.Sc. degrees in 1977 and the D.I.C. and Ph.D. degrees in 1980, all in electrical engineering, from Imperial College, University of London, U.K.

Since 2003, he has been with the School of Electrical and Electronic Engineering, Nanyang Technological University, Singapore, where he is currently a Professor. From 1980 to 1982, he was a National Research Council Research Associate in the Naval Postgraduate School, Monterey, CA. From 1982 to 2003, he was with the Department of Electrical Engineering, National University of Singapore. His research interests include digital signal processing and VLSI circuits and systems design.

Dr. Lim was a recipient of the 1996 IEEE Circuits and Systems Society's Guillemin–Cauer Award, the 1990 IREE (Australia) Norman Hayes Memorial Award, 1977 IEE (U.K.) Prize and the 1974–1977 Siemens Memorial (Imperial College) Award. He served as a Lecturer for the IEEE Circuits and Systems Society under the distinguished lecturer program from 2001 to 2002 and as an Associate Editor for the IEEE TRANSACTIONS ON CIRCUITS AND SYSTEMS from 1991 to 1993 and from 1999 to 2001. He has also served as an Associate Editor for Circuits, Systems and Signal Processing from 1993 to 2000. He served as the Chairman of the DSP Technical Committee of the IEEE Circuits and Systems Society from 1998 to 2000. He served in the Technical Program Committee's DSP Track as the Chairman in IEEE ISCAS'97 and IEEE ISCAS'00 and as a Co-Chairman in IEEE ISCAS'99. He is the General Chairman for IEEE APCCAS 2006 and a General Co-Chair for IEEE ISCAS 2009. He is a member of Eta Kappa Nu.

Dong Shi (S'07) received the B.Eng. degree in electronic engineering from Shanghai Jiaotong University, Shanghai, China, in 2006. He is currently working towards the Ph.D. degree at Nanyang Technological University, Singapore.

His current research interests are low power and low-complexity digital filters design and implementation.